

Multi-Objective Parameter Dependencies in the Design of Ground Source Heat Pump Systems

Sebastian Weck-Ponten, Jérôme Frisch, Christoph van Treeck

Institute of Energy Efficiency and Sustainable Building E3D, RWTH Aachen University

ABSTRACT

This paper investigates the parameter dependencies in the design of ground source heat pump systems (GSHPs) for heating and domestic hot water purposes. Based on parameter studies using the system configurator GeoWPSys+Web, the system interrelationships in the design of GSHPs are analyzed with regard to technical, energetic, economic and ecological evaluation parameters. The cost-effectiveness and the ecological evaluation parameters are highly dependent on the building's energy demand and on the seasonal coefficient of performance (SCOP). Economic savings of a GSHPs compared to a gas condensing boiler (GCB) mainly depends on the investment costs as well as on the gas and electricity prices and

their annual increases. In addition to economic and technical variation options, GeoWPSys+Web can also map influences on CO₂ emissions of the GSHPs. For example, the CO₂ emissions of the monovalent reference case can be more than halved over a period of 20 years with an increased feed-in of renewable electricity into the German electricity mix and a resulting annual reduction of the CO₂ equivalent for electricity by 10%.

Keywords: Planning dependencies, shallow geothermal energy, ground source heat pump systems, system configuration, system configurator, system design, heat pump

INTRODUCTION

GSHPs can play a central role in boosting the heat transition and the decarbonization of the heating sector. However, the expansion of

shallow geothermal systems is stagnating due to an acute shortage of craftsmen and drilling companies, high investment costs, and a complex planning and approval process. In the planning of GSHPS, different methods and tools are used, various planning trades are involved and a variety of design parameters exists that influence each other [1].

Many studies on GSHPS examine an optimal design of the geothermal source system (GSS) in terms of economics (see [2], [3], [4], [5], [6], [7]) or the heat pump efficiency (see [3],[8],[9], [10], [11], [12]) or other evaluation parameters (see [4], [6]). These studies usually focus on subsurface properties, the depth of borehole heat exchangers (BHE), their geometrical dimensions as well as the geometrical layout of BHE fields. Some of them ([3], [8], [13], [7]) also consider groundwater flows.

Economic relationships between the design of the heat pump (HP), its operating mode and connected buffer and DHW storage tanks are often not examined. The majority of the considered studies mainly use static profitability calculations (see [2], [3], [4], [6]) such as investment costs. Dynamic methods such as the net present value (NPV) method are rarely used (see [5], [7]). None of the economic analyses of the considered studies account for variations of dynamic economical

parameters such as the calculation interest rate and price increase rates.

In addition, holistic analyses that include not only economic parameters but also ecological evaluation parameters such as CO₂ emissions are often not carried out.

The objective of this paper is to examine technical, energetic, economic and ecological parameter dependencies in the design of brine-to-water HPs together with BHE, buffer and DHW storage tanks. This study focuses on the design of the HP system (HP as well as buffer and DHW storage tanks) and its effects on the required BHE length as well as on economics and CO₂ emissions of the entire system.

TECHNICAL SYSTEM RELATIONSHIPS

Figure 1 shows the complex technical system relationships of a GSHPS for heating and DHW purposes. In addition to the subsurface properties, the size of the GSS depends on the energy requirements for heating and DHW as well as on the peak loads extracted from the ground. The peak loads are influenced by the annual building energy demands, the size of buffer and DHW storage tanks, the thermal storage capacity of the building and the efficiency of the HP at the respective operating points. Latter is dependent on the supply

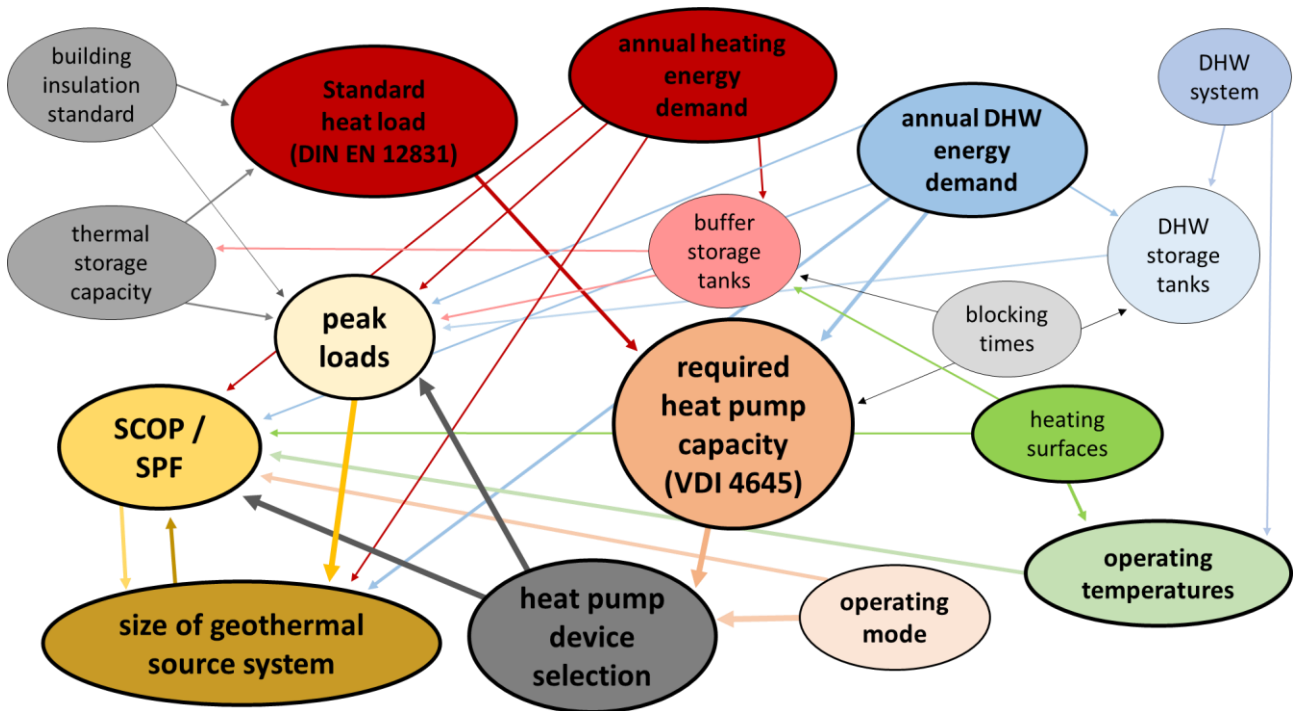


Figure 1: Technical system relationships in the design process of a GSHPs for heating and DHW purposes (based on [1])

temperatures for heating and DHW, the HP's operating mode and the selected HP device. The supply temperatures depend on the heating surfaces (panel heating or radiators) and on the DHW system.

The HP device has a specific coefficient of performance (COP) and nominal capacity in the design point. Based on the operating mode of the HP and the calculated required HP capacity (RHPC) according to the German guideline VDI 4645, a suitable HP device is selected. In the case of a purely electric operation (in Germany defined as the mono-energetic operating mode), the HP can usually be designed smaller, since an electric heating element covers the peak loads. The proportion of the heating element in the total annual

energy consumption has an influence on the seasonal performance factor (SPF; measured value) and on the SCOP (calculated value).

The RHPC is calculated based on the standard building heat load ($\dot{Q}_{H,AP}$), the daily energy demand for DHW ($Q_{DP,ges}$), the hours of a day (d), the sum of blocking times of the HP (t_{SD}) and other energy demands (Q_{misc}), e.g. for heating a swimming pool, according to [14] with the following equation:

$$RHPC = \frac{d \cdot \dot{Q}_{H,AP} + Q_{DP,ges} + Q_{misc}}{d - \sum t_{SD}} \quad (1)$$

The standard heat load depends, among other things, on the building insulation standard and the thermal storage capacity of the building.

SYSTEM CONFIGURATION

The system interrelationships highlight the need for tool-based planning aids such as the web-based system configurator GeoWPSys+Web. The first version of the system configurator was based on an Excel-tool described in [15]. The tool has been further developed and implemented as a Web-Frontend. GeoWPSys+Web allows a detailed configuration of brine-to-water HPs as well as buffer and DHW storage tanks based on real manufacturer component data. The HP as a single heat generator (in Germany defined as monovalent operating mode) and hybrid HP systems (in Germany defined as bivalent operating modes) are compared with a GCB.

As a first approach, the total length of the BHE (l_{BHE}) is calculated in GeoWPSys+Web in a simplified way using the HP evaporator capacity (\dot{Q}_{Eva}) exceeded from the subsurface and the specific BHE heat extraction rate (\dot{q}_{BHE}) according to [16]:

$$l_{BHE} = \frac{\dot{Q}_{Eva}}{\dot{q}_{BHE}} \quad (2)$$

\dot{Q}_{Eva} is determined depending on the design point, taking into account the temperature levels of the heat source and sink side. \dot{q}_{BHE} is a user input dependent on the soil properties at the given project location. In future, the BHE length will be determined based on

simulations using bidirectionally coupled subsurface and HP models.

GeoWPSys+Web uses the NPV method to determine the profitability according to [17] using the following equation:

$$K = -I + \sum_{t=1}^{t_{end}} z \cdot (1+j)^{t-1} \cdot (i+1)^{-t} \quad (3)$$

The negative investment costs of each component (I) are added to the sum of the time-dependent (t in years) incoming and outgoing difference payments compared to the reference system (z) (e.g. energy costs for electricity and gas, costs for CO₂ or replacement investments) considering price increases (j) and the calculation interest rate (i). The investment costs include, among others, HP devices, buffer and DHW storage tanks, GCBs, circulation pumps, expansion vessels and a chimney in case of a GCB. The energy costs for electricity and gas result from the final energy demand, the generator efficiencies (SCOP or boiler efficiency) and from the costs for electricity and gas including price increases. The electricity and gas costs take into account basic costs and a variable price depending on the amount of energy.

The calculation of the SCOP according to the German guideline VDI 4650 is fully implemented in GeoWPSys+Web and takes into account the coverage shares of the

individual heat generators in hybrid operation and the respective DHW share of the final energy demand. Latter results from the useful energy requirement for heating and DHW as well as from heat losses from buffer and DHW storage tanks, heating transfer and distribution losses and the generator efficiencies.

The CO₂ emissions and primary energy demand are calculated based on the final energy demand, the CO₂ equivalents and the primary energy factors for electricity and gas. The CO₂ equivalents and primary energy factors can be adjusted for each year of the observation period. Further information about the economic calculations as well as the CO₂ emissions and primary energy demand calculations is described in [1].

The effects of parameter changes are displayed for all system variants simultaneously and immediately in the web-frontend using diagrams, tables and evaluation parameters. In addition, GeoWPSys+Web gives automated system recommendations and numerous assistance options for the user by calculations running in the background and default values for a maximum number of planning parameters.

GeoWPSys+Web is integrated into a multi-level planning tool consisting of a web-based geoportal including databases, building calculation tools, the open source black-box

characteristic curve HP system model ModHPS [18] and subsurface models. This enables a system design combined with GIS-based analyses including semi-automatic data aggregation and the determination of hourly building load curves. In addition, investigations of mutual interactions between neighboring BHE are possible via a bidirectionally coupled HP and subsurface simulation considering groundwater flow. The area of application of the multi-level planning tool ranges from individual buildings to urban districts. More information about the multi-level planning tool is described in [1].

RESULTS

The following parameter studies are performed using GeoWPSys+Web and focus on basic parameter relationships, the economic considerations, the CO₂ emissions and the primary energy requirement. When purchasing discounted heat pump electricity tariffs, electric suppliers may block heat pumps at certain times. Table 1 lists the impact of blocking times of the HP on the RHPC. The parameter f corresponds to the denominator of Equation 1 (see Equation 4). Due to blocking times, the HP has to be designed up to 33% larger.

$$f = \frac{1}{d - \sum t_{SD}} \quad (4)$$

Table 1: Influence of the blocking times on the calculation of the RHPC

$\sum t_{SD}$	f	%
0	0.042	0
1	0.043	+4.35
2	0.045	+9.09
3	0.048	+14.29
4	0.050	+20.00
5	0.053	+26.32
6	0.056	+33.33

The choice of a larger HP device affects its evaporator capacity at the design point, i.e. the capacity that needs to be extracted from the

subsurface at peak load. Thus, the required size of the GSS also increases with longer blocking times (see Equation 2).

Table 4 in the Appendix lists the boundary conditions of the reference case of the parameter studies. Figure 2 shows the results of GeoWPSys+Web for the reference case.

The energy requirements of the building and the SCOP are crucial variables for economic analyses and ecological considerations. GeoWPSys+Web determines the SCOP_{HPS} of the GSHPS according to [19] which includes the HP, the circulation pump of the GSS and an electrically operated peak load heat generator in a mono-energetic case.

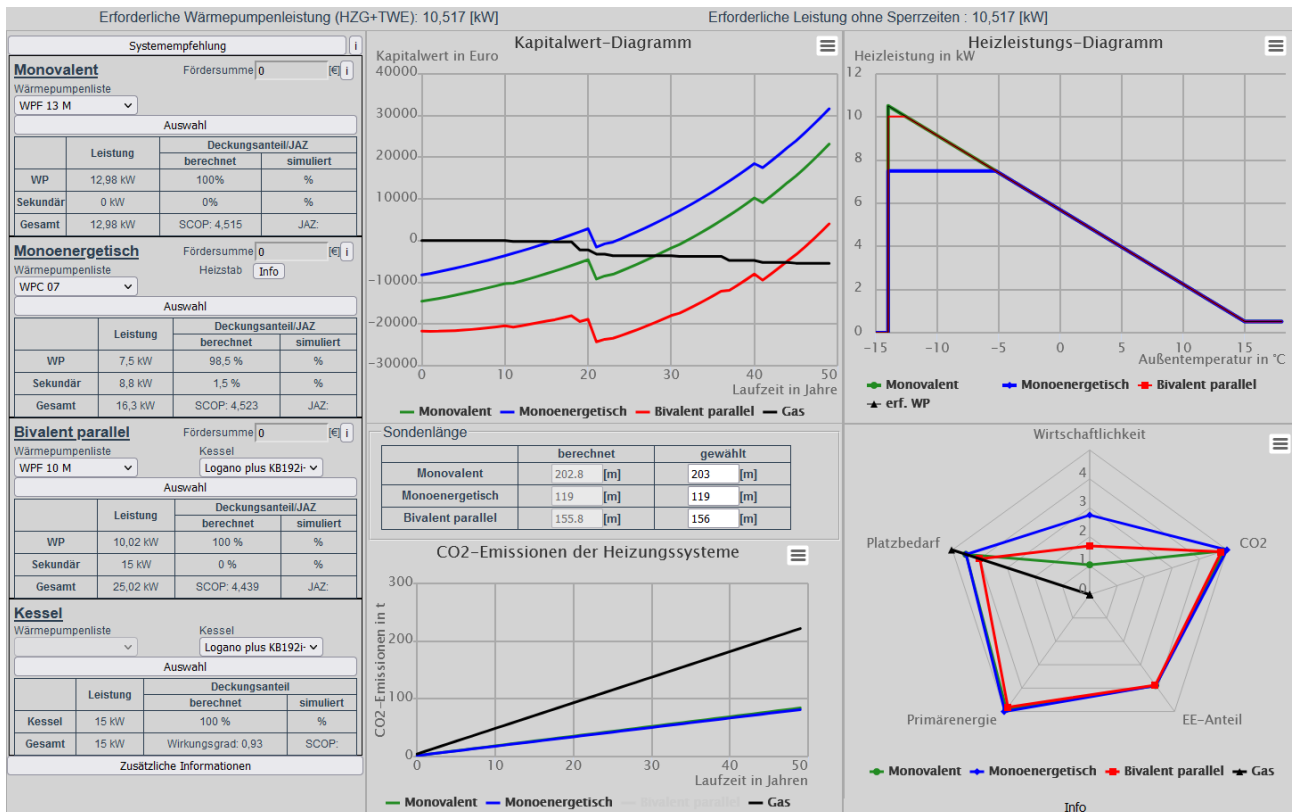


Figure 2: Overview of the results of GeoWPSys+Web of the reference case

The supply temperatures for heating (T_h) and DHW (T_{DHW}) have a significant influence on the different SCOPs of the monovalent reference case (MRC) (see Equations 5-7, Tables 2-3 and Table 5).

Table 2: SCOP_h as a function of T_h and the percentage deviation of SCHOP_h of the MRC (HP unit WPF 13 M)

T_h	F_ϑ	SCOP _h	%
30	1.214	5.361	+5
35	1.157	5.109	0
40	1.099	4.853	-5
45	1.041	4.597	-10
50	0.982	4.336	-15
55	0.921	4.067	-20

Table 3: SCOP_{DHW} as a function of T_{DHW} and the percentage deviation of SCHOP_{DHW} of the MRC (HP unit WPF 13 M)

T_{DHW}	F_1	SCOP _{DHW}	%
50	1.000	3.522	+9
55	0.919	3.237	0
60	0.852	3.001	-7

The SCOP_{HPS} of the MRC can deviate from +3.3% to -16.7%. In the best and worst case, the energy costs in the first year under consideration are 1,524 € and 1,851 €, respectively, compared to the gas costs of the GCB of 1,628 €.

The SCOP depends, among others, on the proportion of DHW in the total heat demand (y), the coverage of the HP in mono-energetic operating mode in terms of space heating and DHW (α) as well as different correction factors ($F_{\Delta\vartheta}=1$, F_ϑ , $F_p=1.035$ for preliminary planning, F_1 as well as $F_2=0.764$ for storage tanks with internal heat exchanger).

If F_p is not selected for the preliminary planning when calculating the SCOP_{HPS} but instead is calculated using the power of the heat source circulation pump (95 W [20]) in the MRC, the SCOP_{HPS} increases by 2.7%. However, the power of the heat source circulation pump is not always included in the manufacturer data sheets.

In GeoWPSys+Web, complex relationships in the design of GSHPS can be displayed and analyzed. For example, the nominal capacity of the HP and the length of connected BHE can be dimensioned smaller if the HP is operated in a mono-energetic operating mode instead of a monovalent operating mode.

The coverage ratio of the heating element has a significant impact on the HP's SCOP_{HPS} (see Table 6) and, thus, on its electric power requirement, annual energy costs, CO₂ emissions and the primary energy of the overall system (see Figures 3 and 4).

$$SCOP_{HPS} = \frac{1}{(1-y) \cdot \frac{\alpha}{SCOP_h} + y \cdot \frac{\alpha}{SCOP_{DHW}} + 1 - \alpha} \quad (5)$$

$$SCOP_h = \frac{COP \cdot F_{\Delta\vartheta} \cdot F_{\vartheta}}{F_P} \quad (6)$$

$$SCOP_{DHW} = \frac{COP \cdot F_{\Delta\vartheta} \cdot F_1 \cdot F_2 \cdot F_{\vartheta}}{F_P} \quad (7)$$

Table 5: $SCOP_h$, $SCOP_{DHW}$ and $SCOP_{HPS}$ of different T_h and T_{DHW} settings and the percentage deviation of $SCOP_{HPS}$ for the MRC

T_h	T_{DHW}	$SCOP_h$	$SCOP_{DHW}$	$SCOP_{HPS}$	%
30	55	5.361	3.237	4.664	3.3
35	50	5.109	3.522	4.634	2.6
35	55	5.109	3.237	4.515	0
35	60	5.109	3.001	4.405	-2.4
40	55	4.853	3.237	4.358	-3.5
45	55	4.597	3.237	4.196	-7.1
50	55	4.336	3.237	4.025	-10.8
55	55	4.067	3.237	3.843	-14.9
55	60	4.067	3.001	3.763	-16.7

Table 6 Impact of the choice of the HP device on the $SCOP_{HPS}$ of the reference case (α : annual coverage of the HP in the annual heat supply; ξ : performance share of the HP nominal heating power (B0/W35) based on the standard heat load)

Name	ξ	α	$SCOP_{HPS}$	%
WPF 13 M	>1	1	4.515	0
WPC 07	0.750	0.985	4.523	0.2
WPF 07	0.750	0.985	4.523	0.2
WPC 05	0.582	0.9528	4.037	-10.6
WPC 04	0.477	0.9016	3.320	-26.5

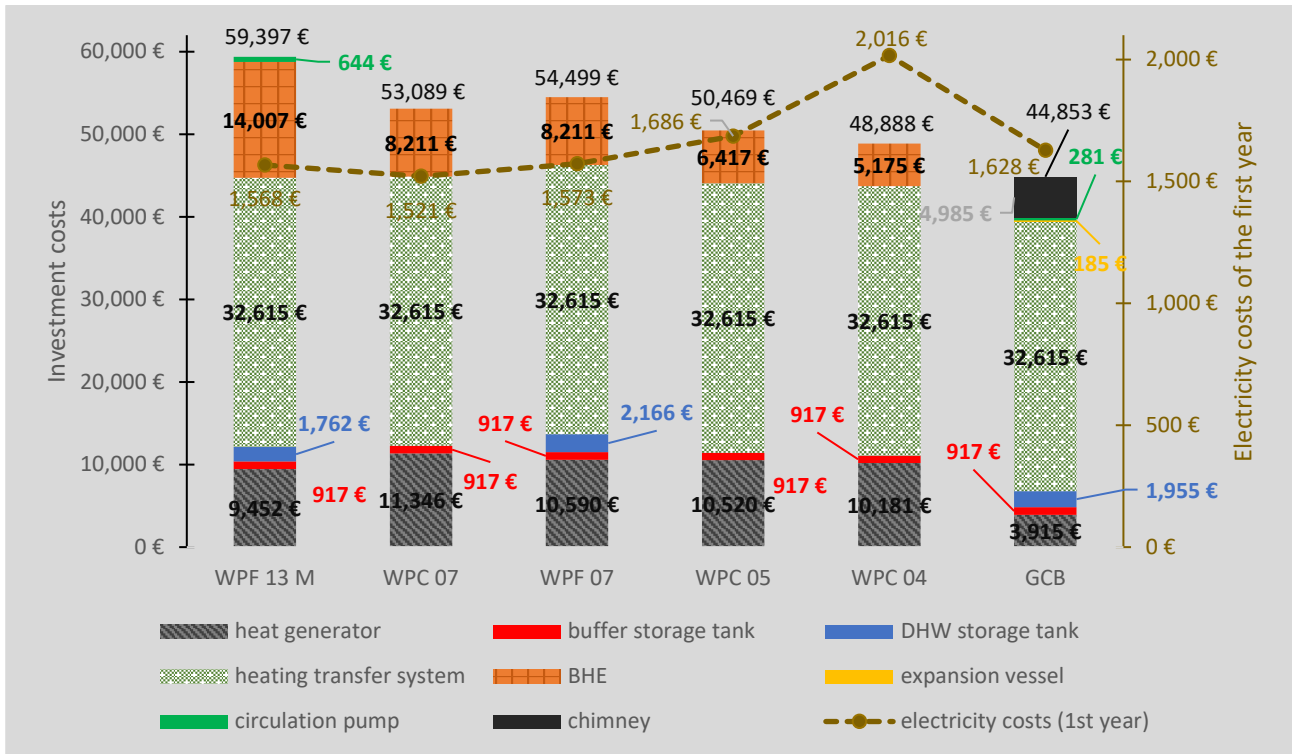


Figure 3: Investment costs (divided according to components) of various mono-energetic GSHPs compared to the MRC and a GCB

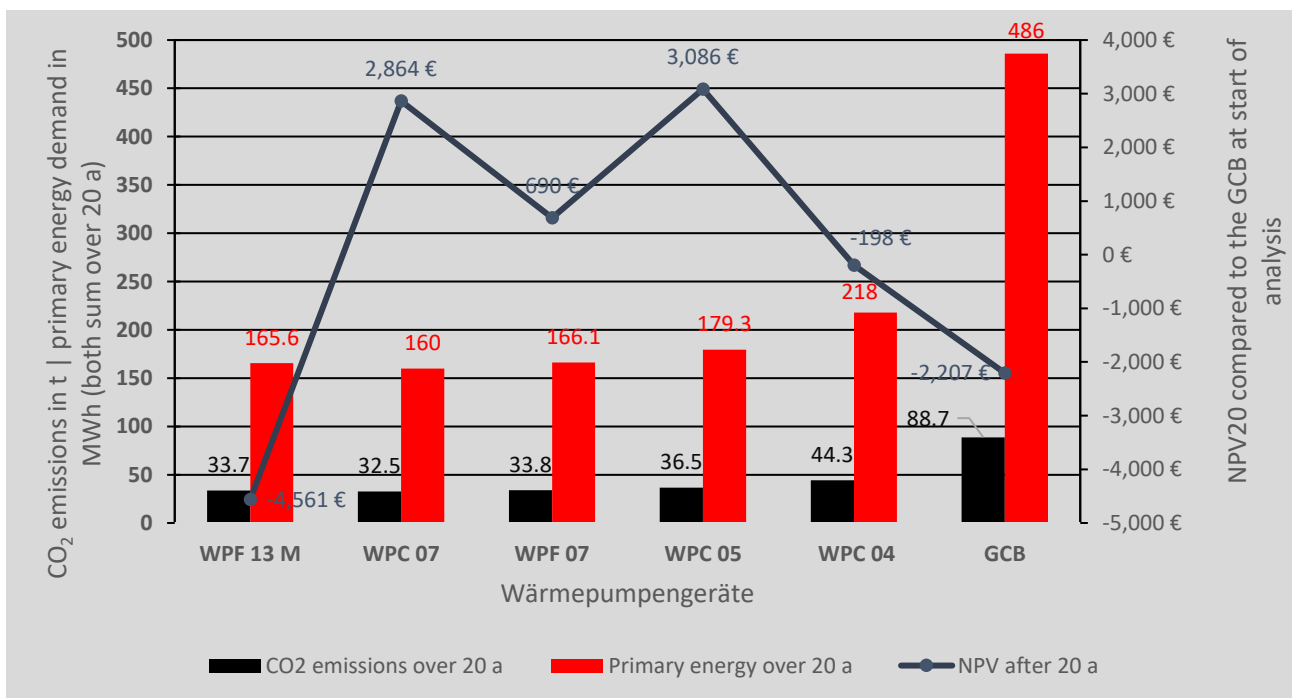


Figure 4: CO₂ emissions and primary energy demands summed over 20 years as well as the NPV20 of the MRC and mono-energetic system variants compared to the GCB at start of analysis (based on [1])

The mono-energetic system with the HP WPC 04 has a heating element share of almost 10%. This reduces the $SCOP_{HPS}$ by 26.5% to a value of 3.32 (see Table 6) and the required BHE length to 119 m compared to 203 m for the monovalent system.

The reduced BHE length and the choice of a smaller HP device also reduce the investment costs for the overall system. The investment costs of the heating transfer system (floor heating), the heat generator and the BHE account for the largest proportion of the investment costs. The share of investment costs for the floor heating system in the total investment costs for the system variants considered amounts to an average of 63%.

On the other hand, the annual electricity costs of the HP rise with the increasing heating element's share of coverage. The HPs of the type WPC have integrated DHW storage tanks. Thus, the DHW storage investment costs and DHW storage heating losses for these HP types do not have to be applied. As a result, the WPF HP types also have lower NPVs compared to the WPC types of the same size (WPF 07 vs. WPC 07).

Furthermore, the NPVs after 20 years compared to the GCB at start of analysis (NPV₂₀) decreases with smaller HPs due to the increasing proportion of heating element.

Figure 5 shows the NPV diagram of the MRC and the HP WPC 04 for the mono-energetic case. In the 16th year of operation, the NPV curve of the WPC 04 is above the curve of the GCB. Thus, the mono-energetic system is more economical than the GCB. The amortization point for the monovalent variant is in almost 27 years. In this form of representation, negative NPVs do not mean that the GSHPS will not amortize.

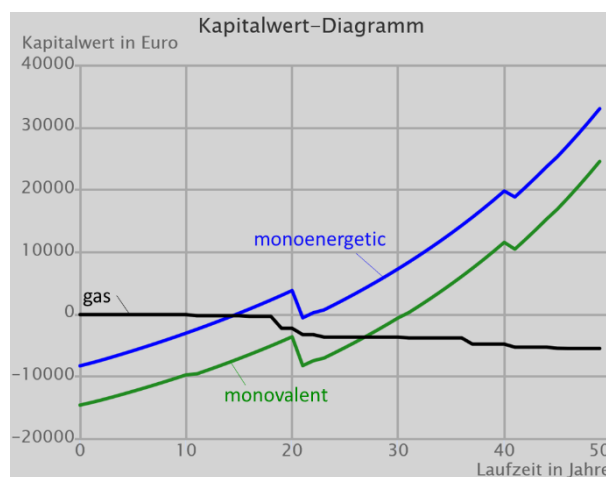


Figure 5: NPV diagram (screenshot of GeoWPSys+Web) of the reference case (monovalent (green) = WPF 13 M; mono-energetic (blue) = WPC 04)

In principle, the choice of the specific HP device and its boundary conditions with regard to other components (e.g. integrated DHW storage tanks) definitely have an influence on the economic efficiency, the CO₂ emissions and the primary energy demands.

The global crises in the recent years have shown that energy prices and cost increases

are difficult to predict. Nevertheless, assumptions have to be made in order to estimate the profitability of projects for a future period. In the reference case, energy prices as well as the investment costs for HPs, other components of the GSHPS and the installation of BHE of the year 2021 are used.

Profitability analyses depend on a large number of parameters. The annual energy demand and the standard heating load of the building, the electricity and gas prices and their price increases, the investment costs and the calculation interest rate as well as government subsidies on the investment costs have a major influence [21].

Table 7 shows the effects on the NPV₂₀ and on the amortization times of the HP WPF 13 M for different energy prices in the period from the year 2021 to 2023. The corresponding NPV diagrams of GeoWPSys+Web also show considerable differences due to the various price sets (see Figure 6).

If a 20% discounted HP electricity tariff of 25.58 ct/kWh and a blocking time of two hours are applied in the energy price set (a), the amortization period is reduced by six years compared to the original variant (a). The RHPC increases from 10.517 kW to 11.473 kW, however, this does not change the HP selection. Larger sized buffer and DHW storage

tanks to bridge the blocking times are neglected in this consideration.

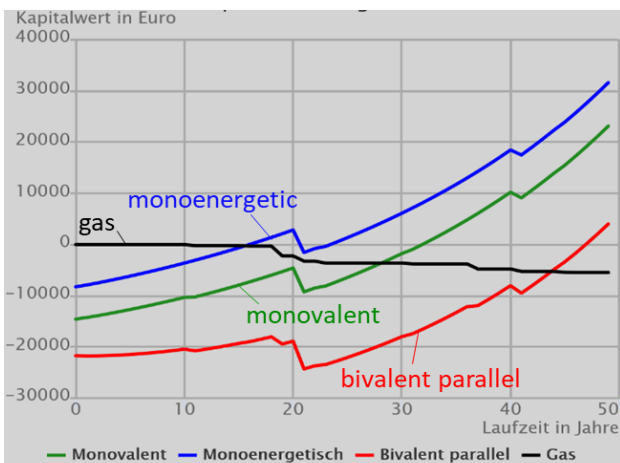
In addition, the variation of the future CO₂ price increase rate (starting in the year 2026) also has a strong impact on the curve shapes and the amortization times (see Figure 7). Higher CO₂ price increase rates favor the economic efficiency of the GSHPS in comparison to the GCB.

In buildings with high heating demands and heating loads, bivalent systems with a GCB can currently also be economically reasonable [21]. The profitability depends on the CO₂, gas and electricity prices and their increases [21]. With regard to the ecological evaluation criteria, the use of a fossil heat generator must be avoided.

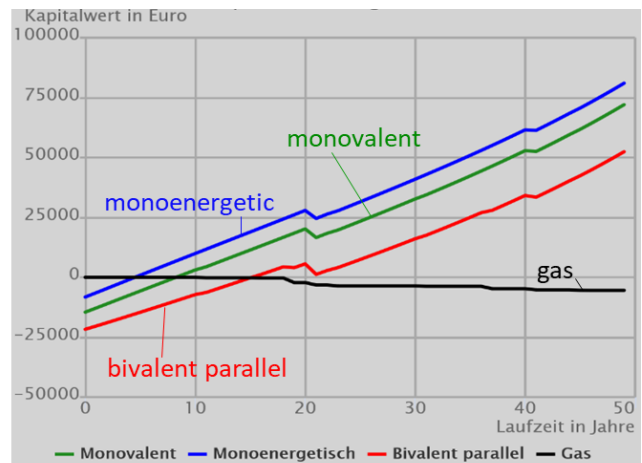
In GeoWPSys+Web, it is possible to reduce the primary energy factors and CO₂ equivalents of electricity and gas for each year of observation. For example, the reduction of the annual CO₂ equivalent simulates an increased feed-in of renewable electricity into the power grid in the future (see Table 8). With increasing CO₂ reduction rates, the CO₂ emissions of the system decrease.

Table 7: Effects on the NPV20 of the MRC for different energy prices

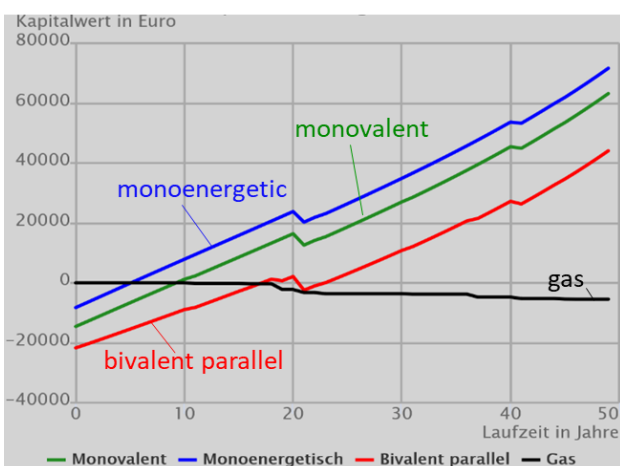
Prices	NPV20	Amortization time in years
Reference case (prices of 2021): gas 6.65 ct/kWh [22] electricity 30.73 ct/kWh [23]	-4,561 €	29
Prices of 2022: gas 16.03 ct/kWh [22] electricity 43.02 ct/kWh [23]	20,198 €	9
Actual prices (31.08.2023): gas 12.5 ct/kWh [22] electricity 30.19 ct/kWh [23]	16,419 €	10
Highest gas price (01.09.2022): gas 40.41 ct/kWh [22] electricity 54.6 ct/kWh [23]	98,295 €	3



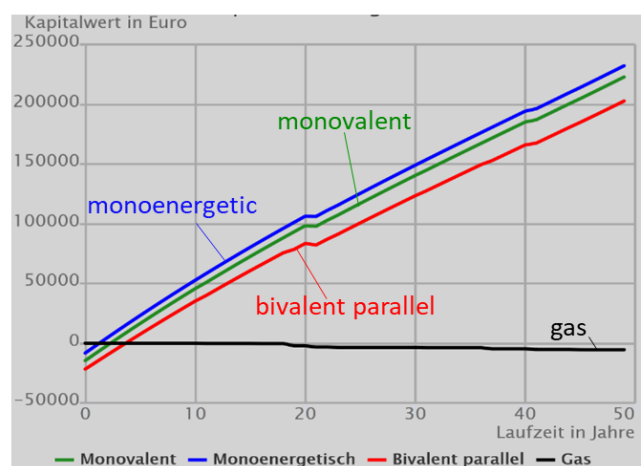
(a)



(b)



(c)



(d)

Figure 6: NPV diagrams of the reference case (monovalent (green) = WPF 13 M; mono-energetic (blue) = WPC 07; bivalent parallel (red)) for different energy price sets (a: prices of 2021 (reference case); b: prices of 2022; c: actual price (31.08.2023); d: highest gas price (01.09.2022)) out of GeoWPSys+Web

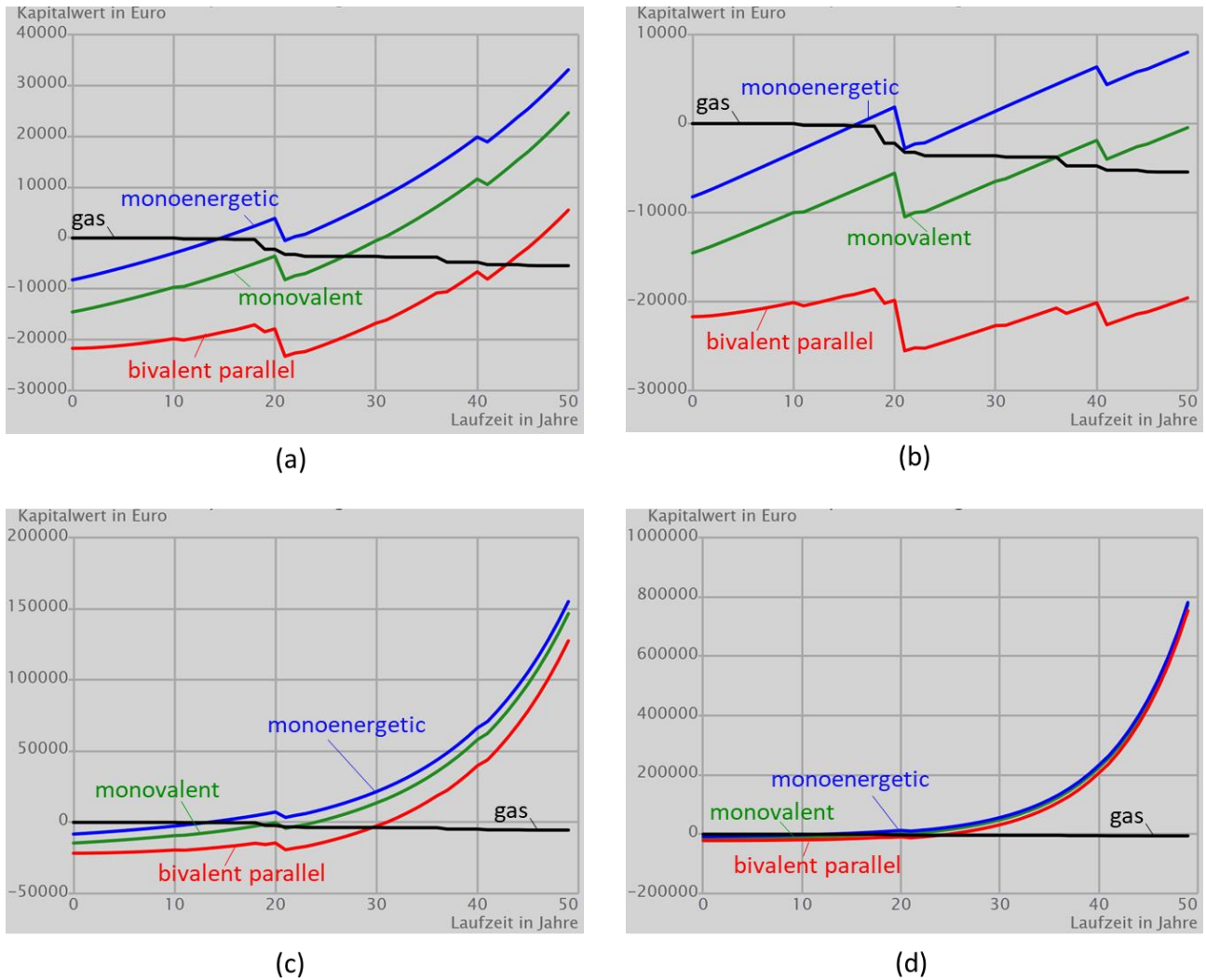


Figure 7: NPV diagrams of the reference case (monovalent (green) = WPF 13 M; mono-energetic (blue) = WPC 07; bivalent parallel (red)) for different annual CO₂ price increase sets (a: 10% (reference case); b: 5%; c: 15%; d: 20%) out of GeoWPSys+Web

Table 8: Effects on the sum of the CO₂ emissions over 20 years (CO₂20) of the MRC for different annual CO₂ equivalent decrease rates of the German electricity mix (CO₂eqEI)

CO ₂ eqEI in %	CO ₂ 20 in t
0	33.66
1	30.65
3	25.60
5	21.60
10	14.79

DISCUSSION AND OUTLOOK

The profitability and the ecological evaluation parameters are highly dependent on the building's energy demand and on the $SCOP_{HPS}$. Thus, the analyses have to be building-specific and component-specific. Economic savings of a GSHPS compared to a GCB mainly depends on the investment costs and the differences in annual energy costs. Latter are in turn dependent on energy prices and their increases. As seen in recent years, forecasts for price increases are subject to a high level of uncertainty. Consequently, price increases should be varied in economic analyses. Regarding the investment costs, catalog prices of 2021 and no end customer prices were used for the devices. The coupling of ModHPS to GeoWPSys+Web allows the verification of important planning parameters, e.g. the $SCHOP_{HPS}$ and coverage ratios. In future work, the effects of bidirectional coupled HP and subsurface simulations on the different evaluation parameters and on the design of the overall system, especially on the calculated size of the BHE, will be investigated.

GeoWPSys+Web is currently being further developed within the project GeoWaermeWende (FKZ: 03EN3059A) [24] with regard to the planning of geothermally

fed low temperature district heating and cooling networks.

REFERENCES

- [1] Weck-Ponten, S. (2023): Simulationsbasiertes Mehrebenen-Planungswerkzeug für geothermische Wärmepumpensysteme; Institute of Energy Efficiency and Sustainable Building E3D, RWTH Aachen University, dissertation 2023
- [2] Blum, P.; Campillo, G.; Kölbl, T.: Techno-economic and spatial analysis of vertical ground source heat pump systems in Germany. In: Energy 36 (2011), pp. 3002-3011
- [3] Casasso, A. and Sethi, R.: Efficiency of closed loop geothermal heat pumps: A sensitivity analysis. Renewable Energy 62 (2014), pp. 737-746
- [4] Huang, S.; Ma, Z.; Cooper, P.: Optimal design of vertical ground heat exchangers by using entropy generation minimization method and genetic algorithms. Energy Conversion and Management 87 (2014), pp. 128–137
- [5] Robert, F. and Gosselin, L.: New methodology to design ground coupled heat pump systems based on total cost minimization. Applied Thermal Engineering 62 (2014), pp. 481-491

- [6] Huang, S.; Ma, Z.; Wang, F.: A multi-objective design optimization strategy for vertical groundheat exchangers. *Energy and Buildings* 87 (2015), pp. 233-242
- [7] Samson, M.; Dallaire, J.; Gosselin, L.: Influence of groundwater flow on cost minimization of ground coupled heat pump systems. *Geothermics* 73 (2018), pp. 100-110
- [8] Casasso, A. and Sethi, R.: Sensitivity analysis on the performance of a ground source heat pump equipped with a double U-pipe borehole heat exchanger. *Energy Procedia* 59 (2014), pp. 301 – 308, European Geosciences Union General Assembly 2014, EGU 2014
- [9] Sivasakthivel, T.; Murugesan, K.; Sahoo, P.K.: Optimization of ground heat exchanger parameters of ground source heat pump system for space heating applications. *Energy* 78 (2014), pp. 573-586
- [10] Sivasakthivel, T.; Murugesan, K.; Thomas, H.R.: Optimization of operating parameters of ground source heat pump system for space heating and cooling by Taguchi method and utility concept. *Applied Energy* 116 (2014), pp. 76–85
- [11] Esen, H. and Turgut, E.: Optimization of operating parameters of a ground coupled heat pumpsystem by Taguchi method. *Energy and Buildings* 107 (2015), pp. 329-334
- [12] Madessa, H.B.; Torger, B.; Bye, P.F.; Erlend, A.: Parametric study of a vertically configured ground source heat pump system. *Energy Procedia* 111 (2017), pp. 1040-1049, 8th International Conference on Sustainability in Energy and Buildings, SEB-16, 11-13 September 2016, Turin, ITALY
- [13] Han, C. and Yu, X.: Sensitivity analysis of a vertical geothermal heat pump system. *Applied Energy* 170 (2016), pp. 148-160
- [14] VDI 4645: Heizungsanlagen mit Wärmepumpen in Ein- und Mehrfamilienhäusern – Planung, Errichtung, Betrieb. 2018. – Verein Deutscher Ingenieure, VDI-Richtlinie
- [15] Weck-Ponten, S.; Eyhusen, D.; Frisch, J.; van Treeck, C.: Systemkonfigurator zur Dimensionierung mono- und bivalenter Wärmepumpen: Teil 1: Systemkonfigurator und Eingabeparameter. In: *HLH-VDI Fachmedien* 72 (2021), no. 01-02, pp. 42–46. <http://dx.doi.org/10.37544/1436-5103-2021-01-02-42>
- [16] VDI 4640 Blatt 2: Thermische Nutzung des Untergrunds – Erdgekoppelte Wärmepumpenanlagen. 2019. – Verein Deutscher Ingenieure, VDI-Richtlinie
- [17] VDI 2067 Blatt 1: Wirtschaftlichkeit gebäudetechnischer Anlagen- Grundlagen und Kostenberechnung. 2012. – Verein Deutscher Ingenieure, VDI-Richtlinie

- [18] Weck-Ponten, S.; Frisch, J.; van Treeck, C.: Simplified heat pump system model integrated in a tool chain for digitally and simulation-based planning shallow geothermal systems. In: Geothermics 106 (2022), 102579. <http://dx.doi.org/10.1016/j.geothermics.2022.102579> – ISSN 0375–6505
- [19] VDI 4650 Blatt 1: Berechnung der Jahresarbeitszahl von Wärmepumpenanlagen. 2019. – Verein Deutscher Ingenieure, VDI-Richtlinie
- [20] JAZ-Rechner des BWP: <https://www.waermepumpe.de/jazrechner/>, zuletzt abgerufen am 12.10.2023
- [21] Weck-Ponten, S.; Eyhusen, D.; Frisch, J.; van Treeck, C.: Systemkonfigurator zur Dimensionierung mono- und bivalenter Wärmepumpen: Teil 2: Parameterstudien und Ergebnisse. In: HLH-VDI Fachmedien 72 (2021), no. 3, pp. 45–49. <http://dx.doi.org/10.37544/1436-5103-2021-03-45>
- [22] Aktuelle Gaspreise für Neukunden: <https://www.verivox.de/gas/gaspreise/>, zuletzt abgerufen am 12.10.2023
- [23] Aktuelle Strompreise für Neukunden: <https://www.verivox.de/strom/strompreisentwicklung/>, zuletzt abgerufen am 12.10.2023
- [24] Drexler, L; Cuypers, L.; Weck-Ponten, S.; Lemmerz, T.; Moubayed, F.; Förderer, A.; Becker, R.; Frisch, J.; Fuentes, R.; Blankenbach, J.; van Treeck, C.: GeoWaermeWende - Empowering Low-Temperature District Heating and Cooling Networks with Comprehensive Geospatial Monitoring, Multi-Purpose Simulation Approaches and User-Centric Planning Tools. In: geoTHERM Journal. 2023

APPENDIX

Table 4: Boundary conditions of the reference case

Parameter	Value
Building type	New building
Standard building heat load	10 kW
Annual energy demand for heating DHW	15,372 kWh 4,530 kWh
Heating limit temperature	15 °C
Blocking times	0 h
RHPC	10.52 kW
HP device (monovalent case)	WPF 13 M
Nominal capacity of the HP device (B0/W35)	12.98 kW
COP of the HP device (B0/W35)	4,57
Supply temperatures for heating DHW	35 °C 55 °C
Buffer storage tank	SBP 200 E
DHW storage tank	SBB 400-1 Plus
Type of thermal heat transfer system	Floor heating
Floor heating area	181 m ²
Investment costs floor heating system	32,615 €
Specific BHE heat extraction rate	50 W/m ²
BHE length	203 m
Specific Investment costs BHE	69 €/m
Total investment costs of the monovalent GSHPs	59,397 €
Total investment costs of the GCB system	44,852 €
CO ₂ equivalents: electricity gas	366 g/kWh 201 g/kWh
Type of electricity tariff	Domestic electricity tariff
Variable portion annual basic costs of the electricity tariff	32 ct/kWh 155 €
Price increase of the electricity tariff (variable portion)	2%
Variable portion annual basic costs of the gas tariff	6.65 ct/kWh 160 €
Price increase of the gas tariff (variable portion)	3%
Price increase of the CO ₂ price	10% (from the year 2025)
Calculation interest rate	5%